Article:
Shu, A., Tang, C., Zhang, X. et al. (2015) Deposition morphology of non-homogeneous debris flow and its energy characteristics. Journal of Mountain Science, 12 (5). 1157 - 1168. ISSN: 1672-6316

https://doi.org/10.1007/s11629-014-3188-9

The final publication is available at Springer via http://dx.doi.org/10.1007/s11629-014-3188-9

R: 20 April 2015
A: 28 May 2015
Citation: Shu AP, Tang C, Zhang X, et al. (2015) Deposition morphology of non-homogeneous debris flow and its energy characteristics. Journal of Mountain Science, 12(5).
DOI: 10.1007/s11629-014-3188-9

Deposition Morphology of Non-homogeneous Debris Flow and Its Energy Characteristics

SHU An-ping [1]*, http://orcid.org/0000-0003-2341-5068; e-mail: shuap@bnu.edu.cn

TANG Chuan [2], http://orcid.org/0000-0001-6942-0976; e-mail: tangc@cdut.edu.cn

ZHANG Xin [3], http://orcid.org/0000-0002-5168-7477; e-mail: lindazhangxin@126.com

SHAO Song-dong [4], http://orcid.org/0000-0001-9952-5293; e-mail: s.shao@sheffield.ac.uk

YANG Kai [5], http://orcid.org/0000-0001-7412-459x; e-mail: yang_k3@ecidi.com

1 Key Laboratory of Water and Sediment Sciences of Ministry of Education, School of Environment, Beijing Normal University, Beijing100875, China

2 State Key Laboratory of Geo-hazard Prevention and Geo-environment Protection, Chengdu University of Technology, Chengdu 610000, China

3 School of Environment, Beijing Normal University, Beijing100875, China

4 Department of Civil and Structural Engineering, University of Sheffield, Sheffield S1 3JD, UK; State Key Laboratory of Hydraulics and Mountain River Engineering, Sichuan University, Chengdu 610065, China

5 Hydrochina Huadong Engineering Corporation, Hangzhou 310000, China

Abstract:
Non-homogeneous two-phase debris flows are widely found in the western mountainous regions of China. To investigate the characteristics of the debris flow deposition process related to the morphology and extent of the debris fan, a series of physical experiments were carried out using an experimental flume. Some useful relationships were obtained to link the flow velocity with the geometric characteristics of deposition morphology and the corresponding area or volume. Based on these, some expressions about energy dissipation process in both the transport-deposition zone and deposition zone are presented, and improved equations describing solid-liquid two-phase energy transformations in the specific deposition zone are also established. These results provide a basis for further investigating the underlying mechanisms of non-homogeneous debris flows, based upon which effective disaster control measures can be undertaken.

Keywords: Non-homogeneous debris flow; Deposition morphology; Debris flow velocity; Energy dissipation

Introduction

Debris flows occur frequently in the western mountainous regions of China during the flood season. These cover an area of 65×10^4 km^2, which accounts for approximately 7% of the land in China. Debris flows in China generally contain gravel, stones, and broken stones as well as tiny clay particles and silt. Non-homogeneous debris flows are characterized by a wide grain size gradation, high volumetric weight, and non-uniformity of both the flow resistance and velocity (Fei and Shu 2004). They behave in a way similar to the properties of the solid-liquid two-phase flows with high sediment transport capacity (Shu and Fei 2008). Furthermore, the deposition, cross-flow, scouring and striking of non-homogeneous debris flows cause a great deal of damage to the local resident and surrounding environment.

The current understanding of debris flow deposition dates back to the particle flow theories put forward by Bag-

nold (1954, 1956). According to this theory, Takahashi et al. (1981) developed debris flow continuum models by analyzing the energy balance of the upper region of debris flows and proposing the concept of debris flow deposition distance. Hashimoto et al. (1990) qualitatively described debris flow depositional substances based on the specific macroscopic and microscopic material characteristics. Quite a few Chinese researchers have also made valuable investigations into the deposition process of debris flows (Liu and You 2006; Qian et al. 2003; Wang 2001; Wang et al. 2001; Yang 2003). For example, Tang and Liu (1993) studied the effects of slope on the morphology of debris flow deposition fans through small-size flume experiments. According to the mechanisms of mudflow movement, Fei and Xiong (1995) summarized different forms of movement of various granules in debris flows and their energy losses. Tang et al. (2012) preliminarily estimated the runout distance and width of the debris flow deposition fan induced by the rainfall using a case study. Wang et al. (1998) assessed the shape of deposits using the indexes of deposition area and maximum deposition length. Vincenzo et al. (2010) proposed an energy-based runout formula to calculate the runout distance of debris flows. Vallance and Scott (1997), Keylock (2005) and Major (1997) also did much experimental work to find out the laws governing runout distance.

Generally speaking, the studies performed to date have well described the characteristics of debris flow depositions, but very limited work has been done to investigate the principles of energy dissipation. Furthermore, most of the available studies were carried out for the homogeneous debris flows, whereas and the results on the non-homogeneous debris flows have rarely been reported. According to the grain size composition and specific gravity of solid materials, debris flows can be classified generally into homogeneous and non-homogeneous flows. The former carries mainly a large amount of fine particles, while the latter consists of both fine particles (silt and clay) and coarse particles (stone, boulder and cobble). Non-homogeneous debris flows cannot be easily described in a quantitative manner because of their unpredictable movement behaviors. Thus additional research should be done from the perspective of energy dissipation mechanisms to facilitate the development of a dynamic model to predict the non-homogeneous debris flows.

Based on the previous work and by taking into consideration the energy dissipation concept, we have conducted a large-scale debris flow simulation experiment in the Chenjiaba Dam area in Sichuan Province to evaluate the parameters and characteristics during the debris flow movement and deposition and investigate the morphological and energy characteristics of these flows. This study leads to the development of several useful empirical expressions relating the flow velocity to the morphology of non-homogeneous debris flow depositions. We also studied the energy evolutions of the transitional zone during the debris flow deposition as well as those of the depositional area under specified situations.

These study results could provide useful information on the designation of the dangerous areas and the design of disaster prevention and control projects related to the non-homogeneous debris flows commonly found in a practical field. The Chenjiaba Dam area is located in an autonomous county of Sichuan Province. We chose this site to carry out the experiment due to its suitable topography for debris flow evolution and easy access to debris flow materials.

1 Experimental Survey

The laboratory experiments to investigate the deposition of non-homogeneous debris flows were carried out using an experimental flume for the large scale debris flows at the State Key Laboratory of Geo-hazard Prevention and Geo-environment Protection at the Chengdu University of Technology.

1.1 Experimental systems

The experimental system consists of four parts: a flow flume, a deposition plate connected with the flume, a water-sand-gravel stirring device and an electrical power control system. The flow flume, in which the two sides are composed of the armored glass, is 18 m long, 0.35 m wide and 0.5 m high. It includes the upper and lower flumes, for which the length and bed slope are 8 m versus 10 m, and 10° ~ 20° versus 3° ~ 12°, respectively. The deposition plate has a bottom slope of 1° ~ 6° and is 6 m long and 4.4 m wide. The experimental system is shown in Figure 1.

1.2 Experimental conditions

‘To reflect as closely as possible the properties of the non-homogeneous debris flows that occurred in the western mountainous area of China, especially in the Sichuan earthquake hazarded areas which happened on May 12th, 2008, the debris flow simulation experiments conducted at Chenjiaba Dam in Sichuan Province were chosen to analyze the mixed silt-sand samples with the same grain size gradation as the field debris flows. The grain size distribution at Chenjiaba was analyzed using the samples found in the source area of this gully, and the gradation summation curve is shown in Figure 2 with the grain size ranging from 0.1 mm to 55 mm. Since this study aimed to analyze the morphological and energy characteristics during the non-homogeneous debris flow deposition, two parameters were investigated in the

experiment: flume slope and volumetric weight of the mixtures. For the experimental system, the slope of the upper flume could vary within a range of 10° ~ 20° and that of the deposition plate could be adjusted from 1° ~ 6°. Additionally, the volumetric weight of the mixtures was set as 1.8 $t \cdot m^{-3}$ and 2.0 $t \cdot m^{-3}$, respectively, so that experimental results could be analyzed under the changes in the volumetric weight value.

1.3 Experimental methods

First, we combined the grains of different sizes to form loose mixtures with the same grain size gradation as those sampled at Chenjiaba. Then we set up the slopes of the upper flow flume and the deposition plate to the required level and moved the materials to a high-speed by using the stirring device with an electrical hoist transportation system. During this process, the materials were continuously stirred to ensure the mixing uniformity. After reaching the downstream gate, the debris flows were released and the deposition morphologies and flow velocities were measured. The experimental conditions are shown in Table 1 and summarized as below:

A．Fixed parameters: upper flow flume (8 m long, 35 cm wide), lower flow flume (10 m long, 35 cm wide and bed slope 10°), deposition plate (6 m × 4.4 m), grain size range (0.002 ~ 55.0 mm)

B．Adjustable parameters:

(1) Upper flow flume bed slope i_1 = 21°, 18°, 15°

(2) Deposition plate slope i_2 = 3°, 5°

(3) Solid grain: volumetric weight with a viscosity of 6% ~ 10% (γ_m = 1.8, 2.0 $t \cdot m^{-3}$)

In order to analyze the relationships between the deposition morphologies, flow velocities and energy dissipations of the non-homogeneous debris flows, we varied the volumetric weight of the mixtures and the slopes of the circulation and deposition zones, based on the above fixed grain size gradation as shown in Figure 2. The purpose is to determine useful relationships among these key parameters for the practical evaluation of debris flow disasters in the downstream areas.

1.4 Measured data

Data was recorded on the geometric morphologies (length, depth and section), dynamic water parameters (flow velocity and mud depth) and grain parameters (e.g. grain size gradation, volumetric weight) during the debris flow deposition process by using the standard measurement techniques. Flow velocities were measured by a real-time flow field measurement system. These measured data (as shown in Table 1) included the deposition form proportion index Cr and the fan angle α, which are respectively expressed as follows:

$$Cr = L_{\max} / W_{\max} \quad (1)$$

and

$$tg\alpha = L_{\max} / D_{\max} \quad (2)$$

where $L_{\max}$ is the maximum deposition length (m), $W_{\max}$ is the maximum deposition width (m), $D_{\max}$ is the maximum deposition depth (m).

To evaluate the data cohesion between the present simulation experiment and the field debris flows, the parameter Froude number Fr was calculated, as shown in Table 2 together with the data of several natural debris flow valleys. The Froude number of the field debris flows varies from 0.804 to 2.436 in typical western regions of China, which is similar to the Froude number in the present experimental study. In this regard, the findings of proposed simulation experiments can be used for the interpretation of field debris flows with reasonable accuracy.

2 Multi-variable Regression Analysis

2.1 Multi-variable regression analysis

The multi-variable regression analysis is a statistical technique that uses several explanatory variables to predict the outcome of a response variable, which takes a group of random variables and tries to find a mathematical relationship between them. The practical implementation of this technique to a particular problem may involve several types of univariate and multivariate analyses in order to understand the relationships between variables and their relevance to the actual problem being studied. This method has been widely used in the engineering field to study the relationships among different influence factors on a main target parameter of interest. The multi-variable regression analysis includes many different kinds of the models, each with its own type of analysis, among which the multivariate analysis of variance is commonly used in hydraulic and sediment engineering.

SPSS is a software package used for the statistical analysis that includes the function to achieve multi-variable re-

gression analysis. The software was originated as the Statistical Package for the Social Sciences (SPSS), but now it is quite popular in other fields as well, including the engineering field as carried in this study. SPSS also includes several software packages for the descriptive statistics, bivariate statistics, predictions of numerical outcomes and group identifications.

In the following, we will use the SPSS software to identify the most influential factors on the debris flow velocity. Due to the limitations of the experiment and other complex issues, the influence factors only include three parameters of two topographic slopes and one volumetric weight. We aim to investigate the most influential factor contributing to the debris flow velocity and quantify the empirical relationships for the test range.

2.2 Debris flow velocity

Debris flow occurs under the proper water, geological and topographical conditions. The water effect in this study is reflected by the volumetric weight and more water leads to lower volumetric weight. The geological condition is reflected by the grain size gradation and viscosity of the mixtures in each experiment, which also changes the volumetric weight. The slopes of the upper flow flume and the deposition plate are adjusted in each experiment to reproduce the topographical condition. In summary, all the measured parameters in this work can be classified as condition parameter and result parameter by following Jiskoot et al. (1998), which is shown in Table 3.

Flow velocity is one of the most important parameters to describe the debris flow movement, and it varies with different debris flow occurrence conditions, including the topographical slope and volumetric weight conditions. According to the multi-variable regression analysis by the SPSS software, the flow velocity U is obtained below:

$$U = 1.733 + 0.124i_1 + 0.01i_2 - 1.383\gamma_m \quad (3)$$

where i_1 is the slope of the upper flow flume (°), i_2 is the slope of the deposition plate (°), and γ_m is the volumetric weight ($t \cdot m^{-3}$).

The results from the regression fitting of above three independent variables are provided in Table 4, where the correlation coefficient is $R = 0.950$. At the 95% significance level, a parameter is regarded as being significant when its value is approximately twice the standard error. In Table 4 the multi-variable linear regression clearly reflects the obvious relationships between the flow velocity U and the other conditional parameters. Among them, the topographical conditions, including the slope of t the upper flow flume i_1 and the deposition plate i_2, exhibit a positive effect, while the volumetric weight shows a negative relation with the flow velocity. Moreover, the volumetric weight contributes more to the change of U.

3 Results and Discussions

3.1 Deposition morphology parameters

In this section we will use the measured geometric characteristics of the deposition morphology under different hydrodynamic conditions to establish the relationships with flow velocity for the non-homogeneous debris flows and then derive the semi-empirical prediction equations and their correlations. Moreover, the empirical expressions will also be established for the amount of the deposition characteristics such as deposition fan area and volume.

3.1.1 Maximum deposition length, width and depth

The relationships between the geometric characteristics, including the maximum deposition length (L_{max}), maximum deposition width (W_{max}) and maximum deposition depth (D_{max}), and the flow velocities (U) are shown in Figure 3.

The above data demonstrate that L_{max} and U exhibit an obvious positive linear correlation, with a correlation coefficient of $R^2 = 0.9198$, which reveals the degree of closeness of the two variables. The empirical expression describing this relationship is:

$$L_{max} = 62.022U + 394.4 \quad (4)$$

W_{max} and U present a clear negative linear relationship, with a correlation coefficient of $R^2 = 0.936$. The empirical expression is:

$$W_{max} = -48.176U + 443.33 \quad (5)$$

Finally, D_{max} and U also show an obvious negative linear correlation, with a correlation coefficient of

$R^2 = 0.946$. The empirical expression is:

$$D_{\max} = -4.237U + 16.30 \quad (6)$$

Based on the above analysis, when U at the end of the circulation zone increases, $L_{\max}$ also increases, but $W_{\max}$ and $D_{\max}$ decrease accordingly. According to the formulation of form proportion index Cr, an increase in $L_{\max}$ and decrease in $W_{\max}$ results in an increase in Cr, which means the debris deposition area becomes elongated.

3.1.2 Deposition area and form proportion

The relationships between the deposition area and flow velocity are shown in Figure 4， as well as those between the deposition form proportion and flow velocity.

Figure 4 demonstrates that the deposition area (S) and flow velocity (U) exhibit an obvious positive linear correlation, with a correlation coefficient of $R^2 = 0.9625$. The empirical expression is:

$$S = 0.375U + 0.781 \quad (7)$$

The deposition form proportion (Cr) also displays a clear positive linear relationship with the flow velocity (U) with $R^2 = 0.8656$, for which the expression is

$$Cr = 1.758U + 8.427 \quad (8)$$

3.1.3 Fan angle and flare

The relationships between the angle of deposition area and the flow velocity for the proposed non-homogeneous debris flows are shown in Figure 5.Based on the data presented in Figure 5, it can be concluded that the fan angle ($tg\alpha$) and flow velocity (U) exhibit an obvious positive linear correlation, with a correlation coefficient of $R^2 = 0.96$. The correlation empirical expression is

$$tg\alpha = 29.36U + 7.500 \quad (9)$$

where $tg\alpha = \frac{L_{\max}}{W_{\max}}$ is used to evaluate the deposition fan angle.

Furthermore, the angle of alluvial fan flare ($tg\frac{\beta}{2}$) and flow velocity (U) present a clear negative linear correlation, with a correlation coefficient of $R^2 = 0.961$. The empirical expression is

$$tg\frac{\beta}{2} = -0.106U + 0.536 \quad (10)$$

where the angle of alluvial fan flare is defined by $tg\frac{\beta}{2} = \frac{W_{\max}}{2 \times L_{\max}}$.

The empirical expression shows the angles of both the deposition fan and the fan flare change with the maximum deposition length, depth and width. Thus these two parameters can provide clear information on the morphology of debris flow depositions under different hydrodynamic conditions.

3.1.4 Deposition area

The experimental results indicated that the deposition area (S) of a non-homogeneous debris flow fan can not be simply represented due to its irregular configuration. For this reason, it can be modeled as the standard fan with a radius of $L_{\max}$ and central angle of β. By using the following simple geometry relationships,

$$S = \frac{n\pi R^2}{360} = \frac{\beta\pi L_{\max}{}^2}{360} \quad (11)$$

the formula representing the area of deposition fan of a non-homogeneous debris flow can be obtained as

$$S = \frac{\pi arctg(-0.106U + 0.536)(62.022U + 394.4)^2}{180} \quad (12)$$

Thus the deposition fan area can be obtained based on the flow velocity used in the experiment, which is shown in Tables 5 and 6 for the two different deposition slopes.

Here it should be noted that when the circulation slope increases, more slurries are washed away; in addition, the dimension of the deposition plate severely limits the measurement of the deposition area. As a result, the corrected re-

sults shown in Table 6 are a necessary modification of the observed results. The above two tables revealed that the errors between the calculated and observed deposition fan areas are within 5%. Thus, Eq. (11) is considered to have good reliability in predicting the debris fan areas.

3.2 Characteristics of energy dissipation

The deposition process of a non-homogeneous debris flow begins at the end of the circulation zone, where the flow energy sharply decreases due to the decrease in the bed slope of the flume and the enlargement section (Wang et al. 1998). Consistent with the conservation of energy principle, the energy dissipation and conversion change significantly: the former increases, whereas the latter decreases. Thus they follow different laws in the deposition zones.

3.2.1 Energy dissipation in transport-deposition zone

The transport-deposition zone of a non-homogeneous debris flow is located between the end of the circulation zone and the beginning of the deposition zone. As the slope of the end flow region is approximately 10°, the energy transition accounts for a large proportion within this zone, whereas the energy dissipation accounts for only a small part.

Prior to the debris flow simulation experiments, a real-time flow field measurement system and a high-precision ultrasonic probe were placed in the transport-deposition zone to monitor the flow velocity and mud depth during the experiment. The movement of casted buoys was used for the comparison with the results obtained from the real-time flow field measurement system. After the experiments, measurements of the mud depth were taken at certain representative locations to evaluate the accuracies of the mud depth obtained with the ultrasonic probe and the experimental data.

The empirical equation that represents the energy of a debris flow contributing to the water phase is as follows:

$$E = \gamma_m Q_{\mathrm{m}} J_m = \gamma_m A U_m J_{\mathrm{m}} = \gamma_m W D U_{\mathrm{m}} J_{\mathrm{m}} \quad (13)$$

where E is the energy (J), A is the area of cross section (m^2), Q is the flow quantity($m^3 \cdot s^{-1}$) and J_m is the energy slope. During the experiment, the slope of the end flow zone was 0.176 and that of the deposition zone was 0.052. Thus the debris flow energy dissipations can be calculated and the results are shown in Figures 6(a) and (b).

The figures show that the energy dissipation increases gradually between the end of the circulation zone and the beginning of the deposition zone. The dissipation law can be expressed by the empirical polynomials. In Figure 6(a), the initial energy *E* decreases when the flow velocity U decreases, but the decreasing rate exhibits some kinds of similarity. Eqs. (13) - (15) correspond to the flow velocity U of 2.03, 1.45 and 0.98 $m \cdot s^{-1}$, respectively. All the correlation coefficients R^2 are above 0.96. Moreover, by comparing the line trends of Figure 6(b) with Figure 6(a), we find out that the energy decreases more quickly for the slope angles changing from 3° to 5°.

$$E = -0.7443L^2 - 0.885L + 39.074 \quad (14)$$

$$E = -1.3929L^2 + 0.7879L + 34.972 \quad (15)$$

$$E = -0.9429L^2 - 0.3114L + 32.34 \quad (16)$$

As shown in Eqs. (13) - (15), the energy *E* has a non-linear correlation with the deposition length L, and it is also not necessarily a quadratic polynomial.

3.2.2 Energy dissipation in deposition zone

During the physical experiment, the slope of the deposition zone was fixed, and the flow energy dissipated as a result of a sharp slope reduction between the flow flume and the deposition plate and the enlargement of deposition section, where the flow started to settle down. The energy dissipations occurred both latitudinally and longitudinally, but this study mainly focuses on the longitudinal characteristics of the energy dissipation.

According to Eq. (12), by using the fixed slope of the deposition zone 0.052, the energy dissipations are shown in Figures 6(c) and (d) along the length direction in the deposition zone. The data demonstrate that the energy tends to dissipate in a linear manner, but more suitable to be represented by the polynomials. Taking Figure 6(c) as an example, the following Eqs. (16) - (18) are respectively used for the flow velocity U of 2.03, 1.56 and 1.45 $m \cdot s^{-1}$. All the correlation coefficients R^2 are also above 0.96.

$$E = -0.5546L^2 - 3.124L + 31.449 \quad (17)$$

$$E = -0.1597L^2 - 5.2416L + 30.323 \quad (18)$$

$$E = -0.1797L^2 - 5.4709L + 29.779 \quad (19)$$

It is worth mentioning here that the empirical expressions as developed above can only be used for the debris flow conditions similar to those in the experiments, which will require further modification and improvement in the practice.

3.2.3 Two-phase energy transformations

During the energy dissipation and transformation in the debris flow deposition process, the non-homogeneous debris flows can be divided into the solid and liquid phases, respectively, according to the division of critical grain size. The energy of the two phases, i.e. solid phase E_s (J) and liquid phase E_l (J) can be expressed as follows:

$$E_s = \gamma_m Q_s J_s = [\gamma_s + (\gamma_s - \gamma) S_{vs}] A U_s J_s \quad (20)$$

$$E_l = \gamma_l Q_l J_l = [\gamma_s + (\gamma_s - \gamma) S_{vl}] A U_l J_l \quad (21)$$

According to the conservation of Energy Principle

$$E = E_s + E_l \quad (22)$$

The energy balance equation can be derived as below:

$$[\gamma_s + (\gamma_s - \gamma) S_v] U_m J_m = [\gamma_s + (\gamma_s - \gamma) S_{vs}] U_s J_s + [\gamma_s + (\gamma_s - \gamma) S_{vl}] U_l J_l \quad (23)$$

where the subscripts m, s and l indicate the debris flow mixtures, solid and liquid phases, respectively. S_v is the concentrations (kg·m^{-3}), and J represent the resistance slopes.

The flow velocity (U_s) and resistance slope (J_s) of the solid phases are expressed as follows:

$$U_s = U_l \left(\frac{S_{vm}}{1 - S_{vs}} - S_{\mathrm{vs}} \right) \quad (24)$$

$$J_{\mathrm{s}} = X S_{vs} \left(\frac{\gamma_s - \gamma_f}{\gamma_m} \right) \tan \alpha \quad (25)$$

For the liquid phases they are expressed as:

$$U_1 = 27.8 \sqrt{\frac{8}{f_m}} \omega_0 \cdot S_{vl}^{\frac{2}{3}} \left(\frac{4R}{d_0} \right)^{\frac{1}{9}} \quad (26)$$

$$J_l = \frac{1}{gR} \left[27.8 \omega_0 S_{vl}^{\frac{2}{3}} \left(\frac{4R}{d_0} \right)^{\frac{1}{9}} \right]^2 \frac{\gamma_f}{\gamma_m} \quad (27)$$

where S_{vm} is the saturation sediment concentration (kg·m^{-3}), X is the quality percentage of the coarse particles (%), α is the friction angle (°), f_m is the resistance coefficient of liquid phases, d_0 is the critical size separating coarse and fine particles (m), ω_0 is the particle settling velocity at critical size d_0 (m·s^{-1}), and R is the hydraulic radius (m).

Therefore, based on Eq. (22) we have studied the relationships of two-phase flow velocities and resistance slopes as shown in Eqs. (23) – (26). Four out of twelve experiments as shown in Table 1 are used to investigate the solid-liquid two-phase energy dissipations and the results are shown in Figures 7(a) - (d).

As demonstrated in the above figures under different debris flow velocities, at a volumetric weight of 1.8 or 2.0 t·m^{-3}, the energy of the liquid phase exceeds that of the solid phase for all the cases and thus it will require a longer distance to dissipate, which is consistent with our previous findings regarding the grain size distributions in the deposition zone (Shu 2010). In this model, the liquid phase predominates in the thin debris flow deposition process and the thin grains constitute a larger part near the front of the deposition zone. These findings reveal the two-phase energy transformations during the deposition process, and provide a scientific basis to establish the dynamic deposition models of non-homogeneous debris flows.

Referring to the work of Jiskoot et al. (1998) and Gray and Kokelaar (2010), the present single and multi-variable analysis among the condition-result parameters could provide useful information to delineate the major factors contributing to the debris flow movement and deposition. The two-phase flow characteristics of the debris flow as observed in the experiment and analyzed through the energy equilibrium theory could be used to build more advanced numerical models and select appropriate phase parameters in practical debris flow simulations.

5 Conclusions

This research mainly focuses on the deposition mechanism of non-homogeneous debris flows which are common in the southwest region of China. Preliminary energy dissipation evaluations are derived. The solid and liquid phases of the debris flow are analyzed according to the two-phase flow theory. In summary, we get the following conclusions:

(1) The multi-variable regression expression between the flow velocity and other conditional parameters is derived. As the topographical condition becomes steeper, the debris flow moves faster. However, the volumetric weight has an obviously negative influence on the velocity.

(2) The maximum deposition length, deposition form proportion, and fan angle exhibit an obvious positive linear correlation with the flow velocity, whereas the maximum deposition width and the angle of alluvial fan flare exhibit a clear negative linear correlation with the flow velocity. Using data fitting, we have established the relationships between the flow velocity and the morphology parameters of non-uniform debris flows, such as the maximum deposition length and width, deposition form proportion, and the angle of the alluvial fan and fan flare.

(3) Irregular deposition fan areas are treated as the standard fans so as to establish the relationships between the fan areas of non-homogeneous debris flows and the flow velocities and deposition volumes based on the depositional characteristics, which is of great practical significance in the designation of dangerous debris flow zones and associated degrees of the disaster.

(4) Based upon the principles of energy dissipation, we have described the energy dissipation process in the transport-deposition zone. Empirical expressions describing the energy dissipations during the debris flow deposition process have also been established, which can serve both as the guidelines to identify the dangerous debris flow zones in order to facilitate the protective designs and as the solid foundations to establish advanced dynamic deposition models for the non-homogeneous debris flows.

Among the conclusions of this research, some can be applied to harness the natural debris flows. For example, the practice of leveling off the gullies can be taken to reduce the topographical slopes, therefore mitigating the debris flow hazards (Kokelaar et al. 2014). However, we should also realize that the present work has some kinds of limitations which need to be addressed in future studies: [1] Due to the experimental devices, the study focused mainly on a limited of key parameters; [2] Only low-density debris flows were investigated, while the energy dissipation mechanisms of high-density debris flows in the deposition zone are still poorly understood; [3] The study site was located in the Jiangjia Valley area, so more refined work needs to be done to predict practical debris flow hazards in other regions; [4] Moreover, diversified surface conditions such as the plant cover, should be taken into consideration when evaluating the evolution of the deposition zone.

Acknowledgements

This work was supported by the National Natural Science Foundation of China (Grant No.11372048, 10972042), National Basic Research Program of China (2011CB403304), Open Fund of Chengdu University of Technology (SKLGP2012K027), Open Fund of State Key Laboratory of Hydraulics and Mountain River Engineering, Sichuan University (SKHL1409) and Open Foundation of the Institute of Mountain Hazards and Environment.

References

Bagnold R (1954) Experiments on a gravity-free dispersion of large solid spheres in a Newtonian fluid under shear. Proceedings of the Royal Society of London 225(1160): 49-63. DOI: 10.1098/rspa.1954.0186

Bagnold R (1956) The flow of cohensionless grains in fluids. Philosophical Transactions of The Royal Society of London, Series A. Mathematical and Physical Sciences A 249(964): 235-297. DOI: 10.1098/rsta.1956.0020

Fei X, Shu A (2004) Movement Mechanism and Disaster Control for Debris Flow. Tsinghua University Press, Beijing. (In Chinese)

Fei X, Xiong G. (1995) Debris flow energy dissipation of sediment transportation and calculation method of velocity of flow and resistance. Journal of Sediment Research 12(4): 1-8. (In Chinese)

Gray J, Kokelaar B (2010) Large particle segregation, transport and accumulation in granular free-surface flows. Journal of Fluid Mechanics 652: 105-137. DOI: 10.1017/s002211201000011x

Hashimoto H (1990) Model of deposition of grains from debris flow. Hydraulics/Hydrology of Arid Lands ASCE

537-542.

Jiang H, Deng Y, Yuan T (2012) Debris flow formation and dynamic characteristics in Jiabagou of Xiaojin County. Ground Water 34(2): 149-152.

Jiskoot H, Boyle P, Murray T (1998) The incidence of glacier surging in Svalbard: evidence from multivariate statistics. Computers and Geoscience 24(4): 387-399. DOI: 10.1016/s0098-3004(98)00033-8

Keylock C (2005) An alternative form for the statistical distribution of extreme avalanche runout distances. Cold Regions Science and Technology 42: 185-193. DOI: 10.1016/j.coldregions.2005.01.004

Kokelaar B, Graham R, et al. (2014) Fine-grained linings of leveed channels facilitate runout of granular flows. Earth and Planetary Science Letters 385: 172-180. DOI: 10.1016/j.epsl.2013.10.043

Liu J, Ou G., You Y (2006) Experimental research on velocity of flow of debris flow and deposition pattern. Research of Soil and Water Conservation 1: 120-123. (In Chinese)

Major J (1997) Depositional processes in large-scale debris-flow experiments. The Journal of Geology 105(3): 345-366. DOI: 10.1086/515930

Qian N, et al. (2003) Mechanics of Sediment Movement. Science Press, Beijing. (In Chinese)

Shu A, Fei X (2008) Sediment transport capacity of hyperconcentrated flow. Science in China Series G: Physics, Mechanics & Astronomy 51(8): 961-975. DOI: 10.1007/s11433-008-0108-4

Shu A (2010) Investigation on movement characteristics for non-homogeneous and solid-liquid two-phase debris flow. Chinese Science Bulletin 55: 3006-3012. DOI: 10.1360/972010-741 (In Chinese)

Takahashi T (1981) Debris flow. Annual Review of Fluid Mechanics 13(1): 57-77. DOI: 10.1146/annurev.fl.13.010181.000421

Tang C, Liu X (1993) Models for dynamic deposition simulation and dangerous area prediction of debris flow. Journal of Soil and Water Conservation 5: 37-40. (In Chinese)

Tang C, Zhu J, Chang M et al. (2012) An empirical-statistical model for predicting debris-flow runout zones in the Wenchuan earthquake area . Quartenary International 250: 63-73. DOI: 10.1016/j.quaint.2010.11.020

Vallance J, Scott K (1997) The Osceola mudflow from mount rainier: sedimentology and hazard implications of a huge clay-rich debris flow. The Geological Society of America Bulletin 109(2): 143-163. DOI: 10.1130/0016-7606(1997)109<0143:tomfmr>2.3.co;2

Vincenzo D, Cesca M, Marchi L (2010) Field and laboratory investigations of runout distances of debris flows in the Dolomites (Eastern Italian Alps) . Geomorphology 115(3-4): 294-304. DOI: 10.1016/j.geomorph.2009.06.032

Wang G, Shao S, Fei X (1998) Debris flow simulation 2: Verification. Journal of Sediment Research 3: 14-17. (in Chinese)

Wang Z (2001) Experimental researches of debris flow tap movement and energy theories. Journal of Hydraulic Engineering 3: 18-26. (In Chinese)

Wang Z, Cui P, Yu B (2001) Movement mechanism and anti-drag of debris flow. Journal of Natural Disasters 10(3): 37-43. (In Chinese)

Yang Z (2003) Analysis on deposition state on debris flow. Chinese Journal of Rock Mechanics and Engineering 22: 2778-2782. (In Chinese)

Yu G, Zhang M et al. (2010) Analysis on the hydrodynamic conditions for the massive debris flow in Sanyanyu based on ArcGIS and DEM. Northwestern Geology 44(3): 53-62. (In Chinese)

Table 1 Conditions and results of the non-homogeneous debris flow simulation experiments

Number	Circulation slope i_1 (°)	Deposition slope i_2 (°)	Volumetric weight r (t·m^{-3})	U (m·s^{-1})	L_{max} (cm)	W_{max} (cm)	D_{max} (cm)	S (m^2)	C_r	$tg\alpha$
1	15	3	2	0.88	446	406	12.5	8.55	1.099	35.68
2	15	5	2	0.95	469	400	12.7	8.62	1.171	36.14
3	15	3	1.8	0.98	453	398	12	8.62	1.138	37.75
4	15	5	1.8	1.02	477	391	11.5	8.76	1.199	39.41
5	18	3	2	1.27	468	384	11.3	8.79	1.219	41.42
6	18	5	2	1.33	481	378	11	8.89	1.286	44.18
7	21	3	2	1.45	480	372	10.6	8.91	1.29	45.28
8	21	5	2	1.52	497	356	10	8.95	1.383	50.2
9	18	3	1.8	1.56	495	370	9.1	9.05	1.338	54.4
10	18	5	1.8	1.67	506	362	8.5	9.06	1.417	58.3
11	21	3	1.8	2.03	530	350	7.8	9.23	1.514	67.95
12	21	5	1.8	1.8	538	345	7.6	9.19	1.617	71.71

* i_1 is the flow flume slope, i_2 is the deposition plate slope, r is the unit weight of debris flow, U is the flow velocity, L_{max} stands for the maximum accumulation length, W_{max} stands for the accumulation width, D_{max} is the maximum accumulation depth, S is the accumulation zone and C_r is the accumulation form proportion.

Table 2 Statistics analysis of debris flow samples in experiments and fields

Category	No. of debris flow observed	Supercritical flow(Fr > 1)	Per.	Subcritical flow (0.7 < Fr < 1)	Per.	Mean Fr number
Present debris flow experiment	12	8	66.7%	4	33.3%	1.265
Field experiments at Jiangjia Valley	10	10	100%	0	0	2.436
Natural debris flow at Jiangjia Valley	8	8	100%	0	0	2.391
Jiaba Valley and its branches in Sichuan Province*	3	3	100%	0	0	1.454
Sanyanyu Valley and its branches in Gansu Province*	3	1	33.3%	2	66.7%	0.804

* Data of debris flow valleys in Sichuan and Gansu Provinces are from references of Yu et al. (2010) and Jiang et al. (2012)

Table 3 Parameters classifications

Condition parameters	**Result parameters**
Volumetric weight r	Flow velocity U
Slope of flow flume i_1	Deposition length L_{max}
Slope of deposition plate i_2	Deposition width W_{max}
	Deposition depth D_{max}
	Deposition area S
	Deposition form proportion index Cr
	Fan angle α

Table 4 Multi-variable SPSS regression analysis of debris flow parameters

Model and parameters	Non-standardized coefficients		Standardized coefficients	*t*	Sig.	95.0% confidence interval for *B*	
	B	STD error	Beta			Lower bound	Upper bound
(Constant)	1.733	0.807		2.147	0.064	-0.128	3.593
Slope of circulation flume i_1	0.124	0.016	0.864	7.807	0	0.087	0.16
Slope of deposition plate i_2	0.01	0.039	0.028	0.258	0.803	-0.08	0.1
Volumetric weight *r*	-1.383	0.388	-0.394	-3.563	0.007	-2.279	-0.488

Table 5 Comparisons of calculated and observed deposition fan areas (deposition slope of 3°)

Flow velocity ($m \cdot s^{-1}$)	0.88	0.98	1.27	1.45	1.56	2.03
Calculated results (m^2)	14.68	14.79	15.05	15.18	15.68	16.38
Observed results (m^2)	14.28	14.55	14.69	14.86	15.22	15.81
Error (%)	2.79	1.66	2.45	2.18	3.04	3.58

Table 6 Comparisons of calculated and observed deposition fan areas (deposition slope of 5°)

Flow velocity ($m \cdot s^{-1}$)	0.95	1.02	1.33	1.52	1.67	2.11
Calculated results (m^2)	8.4980	8.6857	8.7581	8.7484	8.8557	8.8970
Observed results (m^2)	8.62	8.76	8.89	8.95	9.06	9.19
Corrected results (m^2)	10.12	10.76	10.89	11.45	11.56	12.19
Error (%)	1.42	0.85	1.48	2.25	2.25	3.19

Figure 1 Experimental system for debris flow simulation experiment.

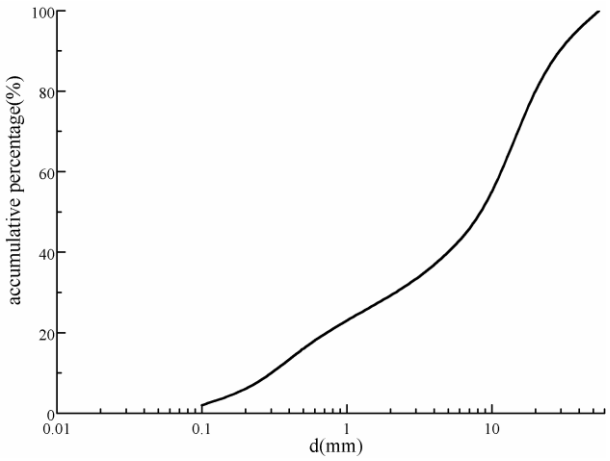

Figure 2 The grain size summation curve of debris flow at Chenjiaba.

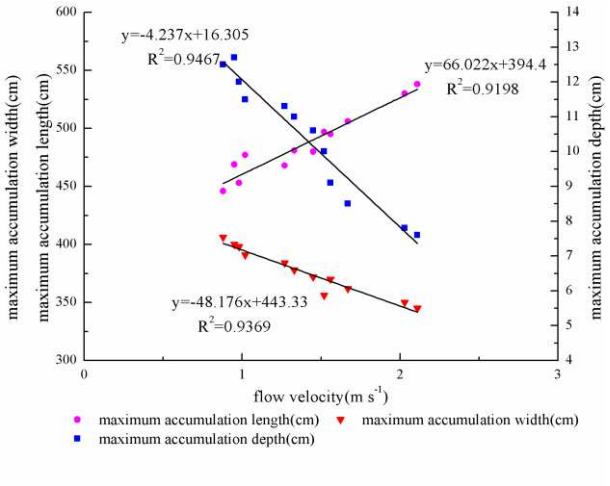

Figure 3 Relationships between geometric characteristics of the debris flow morphology and flow velocity.

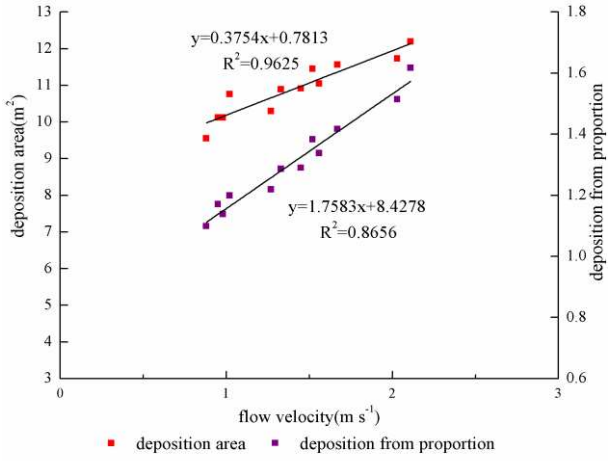

Figure 4 Relationships between deposition area/form proportion and flow velocity.

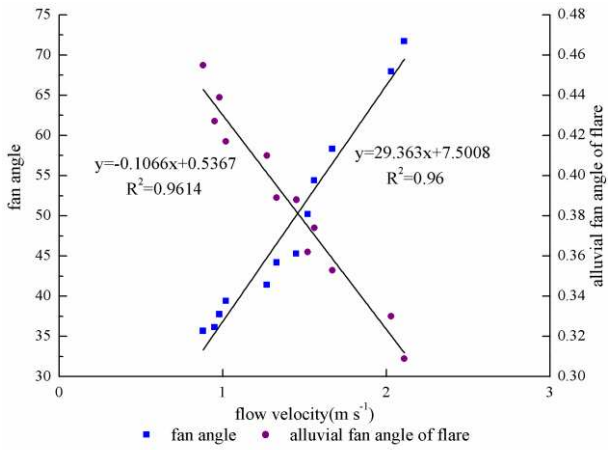

Figure 5 Relationships between fan angle/angle of alluvial fan flare and flow velocity.

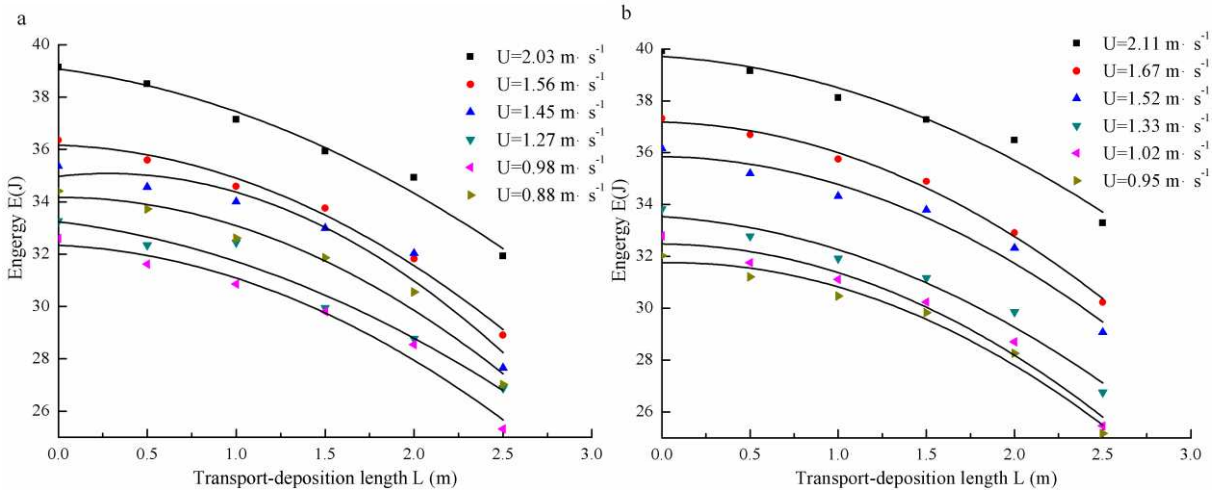

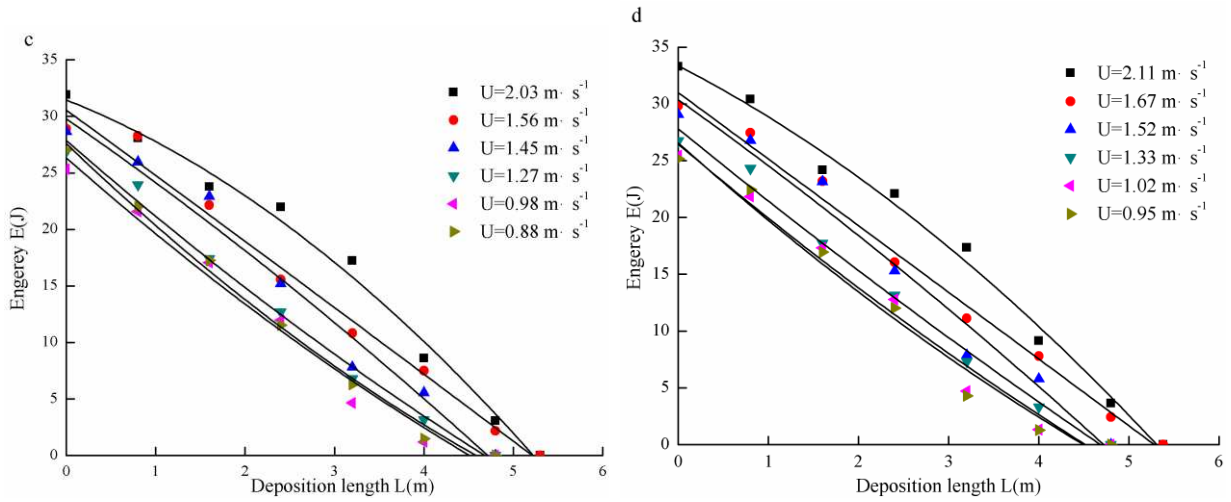

Figure 6 The energy dissipation law of debris flow: (a) transport-deposition zone with deposition slope 3°; (b) transport-deposition zone with deposition slope 5°; (c) deposition zone with deposition slope 3°; and (d) deposition zone with deposition slope 5°.

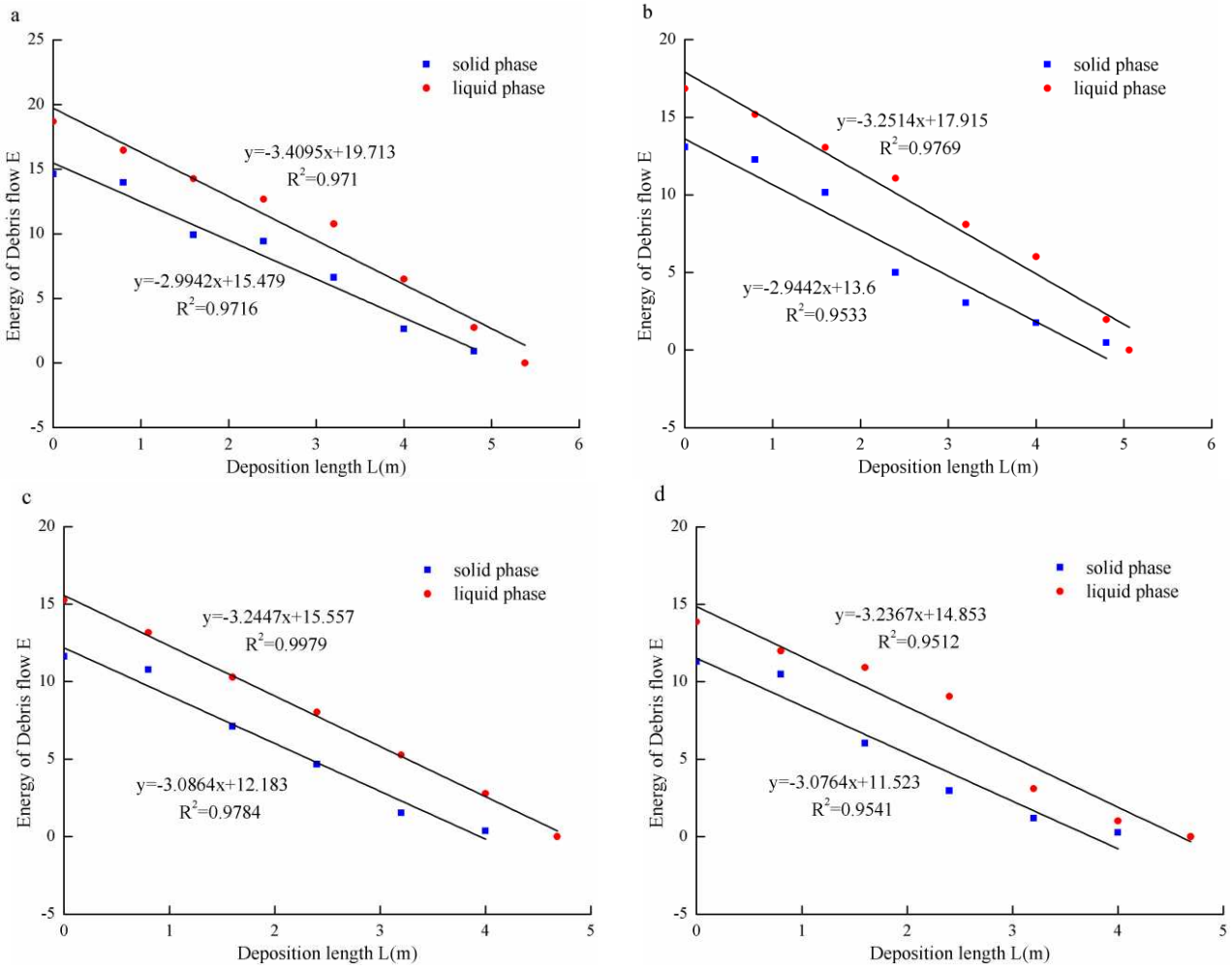

Figure 7 The solid-liquid two-phase energy transformations in the deposition zone under different debris flow velocities *U*: (a) 2.11 m·s^{-1}; (b) 1.67 m·s^{-1}; (c) 1.27 m·s^{-1}; and (d) 0.95 m·s^{-1}